Space Science Reviews (2026) 222:10
https://doi.org/10.1007/s11214-026-01266-x

VISTA: Dust and Volatile Sensor for the ESA Hera Mission

Ernesto Palomba[1] · Fabrizio Dirri[1] · Chiara Gisellu[1,2] · Andrea Longobardo[1] · Vincenzo Della Corte[1] · Enrico Nardi[1,2] · Emiliano Zampetti[3] · Cassandra Montiroli[3] · Diego Scaccabarozzi[4] · Marco Giovanni Corti[4] · Bortolino Saggin[5] · Marilena Amoroso[6] · Margherita Cardi[7] · Marco Pavoni[7] · Daniele Calvi[7] · Andrea Zanotti[7] · Filippo Corradino[7] · Fabio Ferrari[8] · Iosto Fodde[8] · Alessia Cremasco[8] · Paolo Panicucci[8] · Michael Küppers[9] · Patrick Michel[10]

Received: 9 November 2024 / Accepted: 3 January 2026

Abstract
VISTA (Volatile In-Situ Thermogravimeter Analyzer) is a QCM (Quartz Crystal Microbalance) based device designed to characterize the dust environment of the Didymos asteroid system by detecting the presence of dust particles with sizes smaller than 5-10 μm and sub-μm, as well as volatiles and light organics, within the framework of the European Space Agency (ESA) Hera Mission. Thanks to its customized subsystems design, VISTA is capable of monitoring deposition and desorption/sublimation processes in the space environment, as well as molecular contamination (in support to other instruments) originating from outgassing sources during different mission phases, and of performing Thermo-Gravimetric Analysis (TGA) on the collected materials. The VISTA Model development for Hera started in 2020 and continued through 2023, and included an Engineering Qualification Model 0 (EM_0), an Engineering Qualification Model (EQM), a Flight Model (FM) and a Flight Spare (FS). The EM_0 was electrically and mechanically representative of VISTA, while the EQM, FM and FS share the same mechanical structure and electrical connections. The prototype, as well as the Engineering, Flight and Spare Models, were delivered to the prime contractor, Tyvak International. VISTA Models are composed by three different subsystems: two quartz crystals mounted in a sandwich-like configuration; the Proximity Electronics; and the Thermal Control System, which includes two integrated and customized heaters and a Thermo-Electric Cooler to cool the sensor and facilitate dust and volatiles deposition. The VISTA EQM, FM and FS successfully passed the Qualification and Acceptance Test Campaigns. The main results obtained from simulations of particles and volatiles deposition in a vacuum chamber, heating cycles, and Thermo-Gravimetric Analyses are reported in this work.

Keywords Piezoelectric microbalance · Dust · Asteroid · Planetary defence · Hera · Didymos

1 Introduction

The Asteroid Impact and Deflection Assessment (AIDA) international cooperation supports the development, operations and data intepretation of the NASA DART (Double Asteroid

Extended author information available on the last page of the article

Redirection Test) and ESA Hera missions. Its objective is to demonstrate the kinetic impactor concept as a viable technique for deflecting a small asteroid and to characterize the physical properties of the target system. Hera is a Planetary Defence Mission developed within the Space Safety and Security Program of the European Space Agency, and was launched on 7 October 2024 from the Kennedy Space Center. Hera's primary goals include the demonstration of new technologies, ranging from autonomous navigation around a binary asteroid to low gravity proximity operations, the investigation of the Didymos binary system, including the assessment of its internal properties, the characterization of asteroid geophysics (Michel et al. 2022) and the evaluation of the outcome of NASA's DART mission kinetic impactor experiment, which successfully took place in September 2022.

Hera carries two 6U XL CubeSats, namely Milani (Cardi et al. 2026) and Juventas, which will be deployed in close proximity to the Didymos system. Juventas, developed by Gomspace, is dedicated to the geophysical characterization of Dimorphos, while the development of Milani was led by Tyvak International and aims to perform a global mapping of both components of the binary asteroid, with detailed observation of the consequences of the DART impact on Dimorphos. The following payloads are included on board the Milani CubeSat:

- VISTA, a dust and volatile analyser;
- ASPECT, a visible and near-infrared imaging spectrometer;
- NavCam (Navigation Camera), that will provide optical images of Didymos and Dimorphos (Ferrari et al. 2026).

VISTA was developed by an Italian Consortium led by INAF-IAPS (Istituto Nazionale di AstroFisica – Istituto di Astrofisica e Planetologia Spaziali), in collaboration with CNR-IIA (Consiglio Nazionale delle Ricerche – Istituto sull'Inquinamento Atmosferico) and Politecnico di Milano – MetroSpace Lab. The instrument is based on the heritage gained from several ESA ITT-Emits projects:

- CAM (Contamination Assessment Microbalance), developed under the project "Evaluation of an in-situ Molecular Contamination Sensor for space use" (2014-2016);
- CAMLAB (Contamination Assessment Microbalance for LABoratory) developed under the project "Development of a European Quartz Crystal Microbalance" (2017-2019), and CAMLAB 2.0 developed under "European QCM: Bridging from Technical Development to Commercialisation" (2021-2024).

In the context of the Hera mission, VISTA will detect dust in the vicinity of the Didymos system and characterize volatiles and light organics. Dust in the Solar System, such as cometary and asteroidal dust, is considered the smallest building block of planetary bodies, and its characterization provides key insights into the early stages of Solar System formation. Our understanding of the formation and evolution of the Solar System is also constrained by the inventory and spacial distribution of volatiles throughout the system. In particular, the delivery of volatiles of astrobiological interest, such as water and organics, to Earth is a key issue for understanding the origin of life on our planet. Asteroids and comets may have been the source of these volatiles in the atmospheres of the terrestrial planets and in the Earth's oceans (Hartogh et al. 2011). Therefore, the characterization of small bodies is fundamental for studying dust properties, the volatiles fraction associated with dust, dust and ice fluxes, and the dust-to-ice ratio. Furthermore, the near-Earth asteroid Bennu was found to be active by NASA's OSIRIS-REx mission (Lauretta et al. 2019). The origin of observed regular natural ejection of particles from its surface is still not fully understood and may be driven by different processes. One possible mechanism is micrometeorite impacts (Bottke et al. 2020),

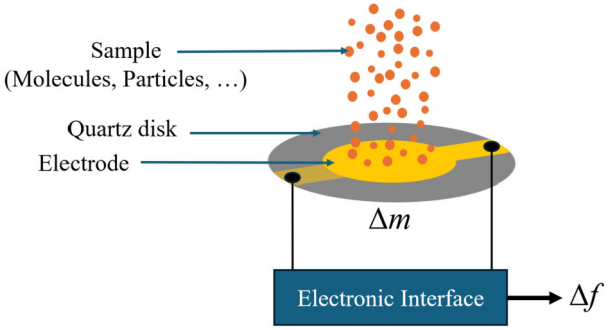

Fig. 1 Working principle of a QCM. The deposited material (e.g. fine dust particles) are collected by the sensitive surface and measured by frequency-mass relation

which should apply to all asteroids, although no previous missions had the same capability as OSIRIS-REx to detect such small ejected particles. In this context, VISTA could provide similar observations and contribute to determining the role of micrometeorite impacts in the ejection of small particles from asteroid surfaces.

2 Quartz Crystal Microbalances

Quartz Crystal Microbalances (QCMs) are widely used sensors in space applications (Dirri et al. 2019), capable of monitoring deposition and desorption/sublimation processes in vacuum (Dirri et al. 2016), in atmospheric conditions (Zampetti et al. 2017, 2008), as well as particles deposition and characterization through Thermo-Gravimetric Analysis (TGA) in various planetary environments (Palomba et al. 2016).

These sensors convert mass changes into fundamental resonance frequency variations, according to Sauerbrey equation (Sauerbrey 1959):

$$\Delta f = -\frac{2f^2}{A_0\sqrt{\rho_q \mu_q}}\Delta m \tag{1}$$

where A_0 is the sensor area, f is the resonance frequency, ρ_q is the quartz density (2.648 g/cm^3) and μ_q is the quartz shear modulus ($2.947{\cdot}10^{11}$ g/cm·s^2). This equation relates the frequency shift of the crystal fundamental resonance to the corresponding mass change. The frequency-temperature dependence is determined by the crystal cut (e.g. AT-cut quartz for VISTA crystals), and its behaviour is correlated to the piezoelectric matrix coefficients.

As depicted in Fig. 1, the QCM sensor consists of a disk of piezoelectric quartz with metal electrodes deposited on its top and bottom surfaces. An electronic interface drives the crystals and converts mass variations, caused by the deposited material (sample), into a corresponding output frequency shift. Typically, this interface includes an oscillator circuit and a digital stage that processes the signal to ensure compatibility with common digital standards (e.g. CMOS, TTL, etc.).

QCM sensors have frequently been employed in space applications to monitor dust flux and volatile outgassing (Palomba et al. 2001, 2002; Wood et al. 1997).

3 VISTA Scientific Goals and Technical Characteristics

VISTA is a μ-thermogravimeter QCM-based device capable of detecting and quantifying the presence of volatile compounds of astrobiological interest, such as water and organ-

ics, in planetary samples. These measurements are particularly relevant when performed on primitive asteroids or comets, as well as on potential targets such as Mars or Jupiter's satellite Europa. Its low mass, volume and power requirements make this type of instrument highly suitable for space missions. Within the framework of the Hera mission, VISTA aims to achieve the following scientific objectives:

- Detect the cumulative mass of dust particles smaller than 10 μm, which may include levitated dust from electrostatic processes, suspended dust within the binary asteroids system, or dust generated by micrometeorites impacts;
- Characterize volatiles (e.g. water) and organics (e.g. low carbon chain compounds) using TGA (Thermo-Gravimetric Analysis) cycles, where the desorption and sublimation rates at specific temperatures are used to identify volatiles and light organics (Langmuir 1913), (Benson and Shaw 1968);
- Monitor molecular contamination from outgassing processes to support other instruments, such as the ASPECT spectrometer.

VISTA can accomplish the first two scientific objectives during the approach, flyby and potential landing on the asteroid. The instrument is positioned in the CubeSat's Field Of View (FOV), aligned with the RAM direction, to maximize the likelihood of accumulating suspended dust within the binary system, or dust lifted by electrostatic processes. The most favorable distance to achieve these first two objectives, i.e. to accumulate dust and volatiles on the piezoelectric element, is between approximately 500 meters and 2 kilometers from the asteroids system, although flybys at these distances can also be effective. The instrument is capable of collecting dust particles even at greater distances, such as 5-10 km from the binary system. The third objective, monitoring molecular contamination coming from outgassing, can be achieved throughout the mission in passive mode, by allowing contaminants such as refractory particles and volatiles to accumulate. The accumulation of contaminants can be further enhanced by using a Thermo-Electric Cooler (TEC) to cool the sensor head by 5-10 °C relative to the surrounding environment. The thermal control of the built-in heaters is managed by the On-Board Software (OBS) through PID controllers, with operations monitored and recorded by the Flight Control Module (FCM).

VISTA technical characteristics are reported in Table 1, and Fig. 2 shows the VISTA Engineering Qualification Model.

4 Design

The instrument core is composed of three separate sub-units packaged in a shielded enclosure.

The first sub-unit consists of two quartz crystals mounted in a sandwich-like configuration. The top crystal serves as the sensing element, exposed to the external environment to collect dust particles from the asteroid system and any outgassed material released during the early mission phases.

The bottom crystal acts as a reference crystal. The output signal is the beating frequency, defined as the frequency difference between sensing and reference crystal. Since the two crystals operate in thermal equilibrium, this differential measurement is, in principle, insensitive to temperature variations.

The second sub-unit is the Thermal Control System (TCS), which drives and regulates the temperature of the crystals. It consists of integrated resistors on the crystals (i.e., two heaters and two temperature sensors) and a Thermoelectric Cooler (TEC). The TCS temperatures

Table 1 VISTA technical characteristics

Characteristics	Value
Crystal resonant frequency [MHz]	10
Mass [g]	90
Volume [mm^3]	79
Sensitive area [cm^2]	1.5
Field Of View [°]	60
Power [W]	<1.5
Data rate [bit/measurement]	96
Particle size detection range	from 5-10 μm to sub-μm particles
PE operational temperature [°C]	from -40 to 60
Crystal operational temperature [°C]	from -150 to 100
VISTA operational temperature [°C]	from -30 to 35
Channels (read-out and controlled)	4 RTDs, 1 frequency, 2 heaters and 1 TEC
Methods/techniques used	1) Dust and contaminants accumulation
	2) TGA cycles
	3) Cooling cycles

Fig. 2 VISTA Engineering Qualification Model

are controlled by the Flight Control Module (FCM) and managed by the On-Board System (OBS). In particular, the TCS enables the crystals to be driven at temperatures up to 100 °C using the heaters, or down -10 °C below the external environment using the TEC, within the Milani mission temperature range.

The third sub-unit is the Proximity Electronics (PE), which includes an oscillator and a beating module.

VISTA temperature can be increased in a stepwise manner to allow the most volatile components of the analyzed sample to desorb. This process, known as μ-Thermo-Gravimetric Analysis, makes it possible to infer the abundance of the desorbed volatile compounds from the measured mass variation, as well as their composition by determining their sublimation temperature and enthalpy of sublimation (e.g. Dirri et al. 2016).

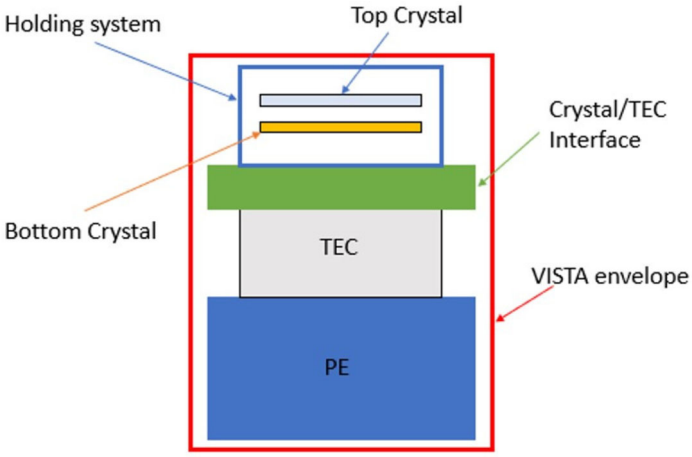

Fig. 3 VISTA mounting concept: the two quartz crystals, mounted in sandwich configuration; the interface plate between the crystals holding system and the Thermo-Electric Cooler (TEC), used to cool down the sensor head with respect to the external environment; and the Proximity Electronics (PE), that manages the output signals (beat frequency and temperatures)

A key challenge of VISTA is the integration of built-in heaters and Resistance Temperature Detectors (RTDs) directly on the crystal surface. The specialized crystals design (Scaccabarozzi et al. 2014) significantly reduces both the instrument mass and power required to perform thermal cycles. Furthermore, characterization of the crystals in low-temperature environments has demonstrated high linearity of the deposited films (Scaccabarozzi et al. 2021) enabling their use in other space missions characterized by wider temperature ranges.

The crystals temperatures are measured with an accuracy of 0.1 °C and a precision of 0.01 °C, while the frequency resolution is 0.1 Hz.

4.1 Thermomechanical Design

The thermomechanical design of VISTA was previously addressed in Scaccabarozzi et al. (2022). In that work, the authors optimized the structural geometry of the instrument by developing finite element models and performing a series of modal, quasi-static, and thermal analyses. These analyses demonstrated both the robustness of the proposed design and its compliance with the mission requirements. Figure 3 illustrates the mounting concept of VISTA, highlighting the main subsystems of the instrument.

In the absence of active thermal control, a temperature difference of approximately 2 °C between the sensing and reference crystals is expected; however, this does not affect the correct functioning of the instrument. When the heaters are activated, the temperature difference becomes negligible, as shown in Fig. 13.

4.2 Proximity Electronic Design

The Proximity Electronics (PE) of the VISTA payload converts mass variations of the working and reference crystals into two electrical signals with resonant frequencies f_W and f_R, respectively. A beating circuit generates the PE output signal, whose frequency corresponds to the difference between the two resonant frequencies:($f_{OUT} = f_R - f_W$). Finally, the PE

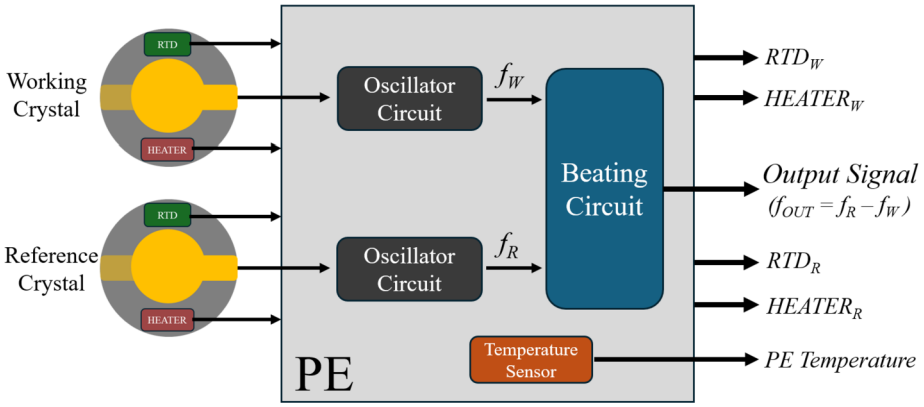

Fig. 4 VISTA PE functional block scheme

includes one RTD (i.e. Pt1000) useful to monitor the PE working temperature. The functional block scheme of the PE is shown in Fig. 4.

The functional block scheme of the Proximity Electronics includes two main blocks. The first consists of two identical oscillator circuits, which convert the electro-mechanical oscillations of the crystals into two electronic signals with frequencies equal to the fundamental resonance frequencies of the crystals. The second block is a circuit that performs the beating between these two frequency signals. The PE output signal is a square wave with a frequency equal to $f_{OUT} = f_R - f_W$. In this way, a mass variation of the working crystal, Δm, is converted into a frequency shift, Δf_{OUT}. This approach exploits the reference crystal to improve robustness against common disturbances affecting both crystals.

The PE board layout was optimized by taking into account components power dissipation, while minimizing the overall volume and reducing electromagnetic interferences. All components used in VISTA PE are Commercial-Off-The-Shelf (COTS) or automotive grade.

4.3 Crystal Design

As previously described, the sensor consists of a thin quartz layer with a pair of deposited electrodes, one on each side. This device is activated through mechanical vibrations induced by applying an electrical voltage to the electrodes. This voltage is supplied by inserting the crystal into a feedback electronic loop (electronic oscillator), as illustrated in the schematic shown in Fig. 5.

The resonant frequency of a quartz crystal can be related to the mass of a deposit layer or particles adhering to its surface (Zampetti et al. 2023). Infact, when the particles are deposited on or attached to the surface of a single crystal, its vibration frequency - typically 10 MHz - decreases. If the attached layer is thin and rigid, the resulting frequency shift is proportional to the mass of that deposition. Under these conditions, the deposited mass can be quantified by applying the Sauerbrey relation (Nivens et al. 1993), which expresses the mass as a function of the crystal intrinsic properties and the measured frequency shift.

VISTA crystals consist of a piezoelectric quartz substrate coated on both top and bottom surfaces with metallic layers that implement three different devices: 1) a pair of metal electrodes (E_A, E_B), 2) a micro-heater, and a 3) micro Resistance Temperature Detector (RTD).

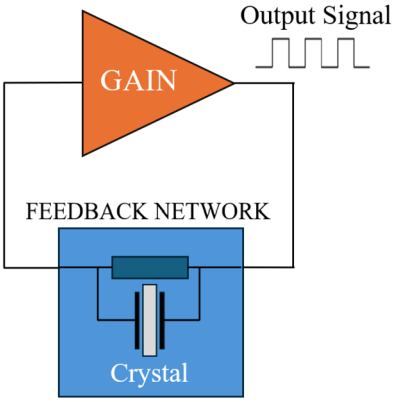

Fig. 5 Crystal is inserted in the feedback network together other passive elements. Generally, the gain block consisted in an amplifier circuit based on transistor, digital gate or operation amplifier

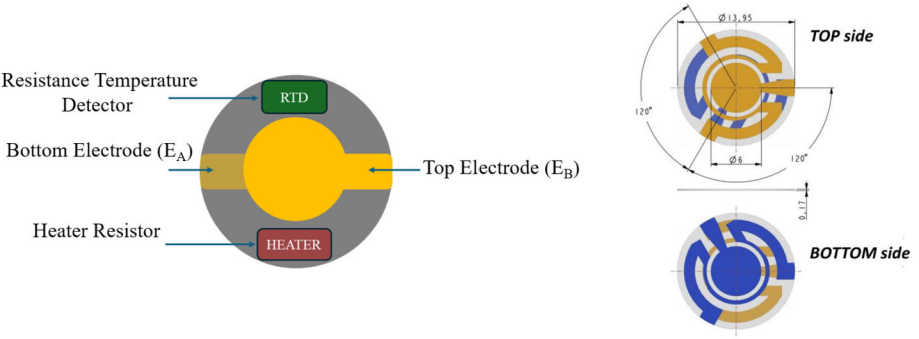

Fig. 6 VISTA crystal sensor schematic (left) and metal structures layout (right). All the reported dimensions are in mm

Table 2 Technical parameters of VISTA crystals

Crystal parameter	Value
Frequency [MHz]	10
Sensitivity [Hz/(g/cm^2)]	$2.2{\cdot}10^{8}$
Inverse sensitivity [ng/(Hz cm^2)]	$4.4{\cdot}10^{-9}$
Thickness [μm]	167
Diameter [mm]	13.95
Roughness [μm]	0.01
Flatness [μm]	<0.2

Figure 6 shows a schematic view of the crystal (left) and the layout of the metal structures (right).

The properties of the quartz slice used to manufacture VISTA crystals are listed in Table 2. In particular, the key properties include the resonant frequency, sensitivity, surface roughness and flatness. The latter two parameters are critical, as they influence vibration damping effects.

VISTA crystals sensors are bi-metal layer structures. In particular, the RTDs, heaters and electrodes consist of two layers: titanium as the first layer and gold as the second. The thin

Fig. 7 Picture of a crystal used for VISTA

titanium layer is primarly used to promote the adhesion of the noble metal (e.g. Au) to the SiO_2 (quartz) surface. Gold is widely employed in microelectronics, and its deposition can be precisely controlled via thermal vapor deposition in a vacuum environment. Moreover, gold is commonly used as a coating due to its unique properties: slow redox processes, high chemical stability, and a favorable thermal resistance within VISTA operational temperature range. In conclusion, the selected materials and fabrication processes are well established and are routinely handled by the research group responsible for manufacturing of the crystal devices (CNR-IIA).

Figure 7 shows an example of the crystals mounted on VISTA. The central area is occupied by the metal electrode, which constitutes the sensitive area of the crystal (A_0). The surrounding Omega-shaped element on the top and bottom electrode is a built-in resistor, functioning as either a heater or a temperature sensor. This layout was chosen to achieve a homogeneous temperature distribution across the crystal, thereby optimizing the performances of the mounting mechanics. Furthermore, the RTDs and heaters share the same layout, which satisfies the device performance requirements while simplifying the production and reducing costs. In commercial crystal sensors, the electrodes have the same layout but are rotated by 180° to facilitate electrical connections. Simultaneously, this ensures that the center of mass coincides with the center of the crystal slice. To interface with VISTA crystals, a dedicated PE circuit was designed and developed to maximize performance while optimizing PCB (Printed Circuit Board) area and minimizing power consumption, thus also reducing overall cost.

5 VISTA Operative Modes and Operations

VISTA Payload can function in different modes:

- **OFF**: the sensor Proximity Electronics (PE) is switched off, and no signals are acquired in this mode. Passive accumulation of dust can still occur and will be measured once the sensor is turned back on;
- **PASSIVE MODE**: the Proximity Electronics is on, the frequency and temperature signals are acquired and monitored. The mas of particles and contaminants is continuously monitored via frequency shifts;

- **ACTIVE MODE - HEATING**: the built-in heaters are used to heat the crystals, for calibration purposes, characterizing the accumulated mass (TGA) and regenerating the crystals;
- **ACTIVE MODE - COOLING**: the TEC is used to cool down the instrument with respect to the external environment.

During the cruise phase, lasting approximately two years, the following activities will be performed, such as:

- health checks, which consist of turning on VISTA and monitoring the beat frequency and the temperatures for 25 minutes;
- calibrations, which consist of heating the crystals with the integrated heaters to obtain the frequency vs. temperature relationship;
- contamination evaluation, which consists of turning on the Thermo-Electric Cooler to cool down VISTA and collect possible contaminants on the sensing crystal.

After arrival at Didymos and Milani deployment in early 2027, VISTA will operate for three months, to characterize the dust environment around the asteroid binary system. In addition to calibrations and cooling of VISTA, long dust accumulation periods (i.e. from days to weeks) are foreseen during the approach to Didymos, alternating with heating cycles with the integrated heaters for the characterization of the accumulated dust and volatiles. In the event of a final landing of Milani on Dimorphos, VISTA will be kept on to continuously monitor the accumulation of dust during this delicate phase.

6 VISTA Test Campaign

VISTA models underwent extensive testing and calibration campaigns, including:

- Calibration tests (frequency vs. temperature), conducted at INAF-IAPS;
- Functionality tests, including frequency stability over time and TCS subsystems tests (INAF-IAPS);
- Performance tests, simulating dust, organics, and volatiles deposition in vacuum to assess instrument mass saturation, mass deposition, and deposition rates as a function of temperature (INAF-IAPS);
- Mechanical and vibration tests, performed at MetroSpace Laboratory, Politecnico di Milano;

A portion of VISTA Test Campaign is presented below, and the main results are discussed.

6.1 VISTA Integration and Qualification Tests

VISTA models were integrated at MetroSpace Laboratory, Department of Mechanical Engineering, Politecnico di Milano, to perform the qualification and acceptance testing under the expected mechanical environment. Prior to the delivery of the Flight and Spare models, the EQM was assembled and characterized under the sweep sine and random vibration levels defined for the unit qualification. The applied vibration levels are listed in Table 3 and Table 4. An electrodynamic shaker (LDS V830), shown in Fig. 8, was used to apply the required vibration levels, and the acceleration of the item was monitored with piezoelectric accelerometers (nominal sensitivity 10 mV/g) mounted on the test unit.

Table 3 Vibration levels - Random excitations (2 min for each axis)

Frequency [Hz]	PSD [g^2/Hz]
20	0.026
50	0.16
800	0.16
2000	0.026

Table 4 Sweep sine levels

Direction	Frequency [Hz]	Qualification load [g]
IP-1	5	1
	18	12
	100	12
IP-2	5	1
	13	8
	100	8
OP	5	1
	13	8
	100	8

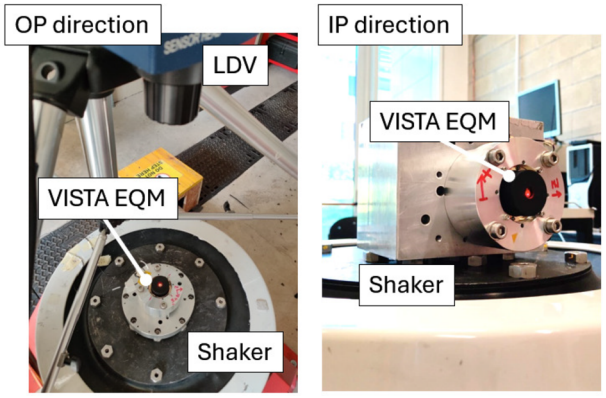

Fig. 8 (Left) The testing setup used in the OP direction testing and (right) testing setup for the IP direction

Before and after each power sine test, a resonance search was performed to verify the mechanical integrity of the tested unit. Additionally, the electrical resistance of the deposited resistors was measured to ensure proper functionality.

Resonance search result for the qualification testing along one directions is given in Fig. 9.

The results indicate that both the electrical resistance measurements and the comparison of the Frequency Response Functions (FRFs) from the resonance search tests showed no anomalies in the behavior of the tested VISTA EQM. Consequently, the EQM mechanical qualification campaign was deemed successful, paving the way to the manufacturing and integration of VISTA Flight Model and Flight Spare. Prior to the delivery to the Milani CubeSat team, both instruments successfully completed the acceptance testing campaign.

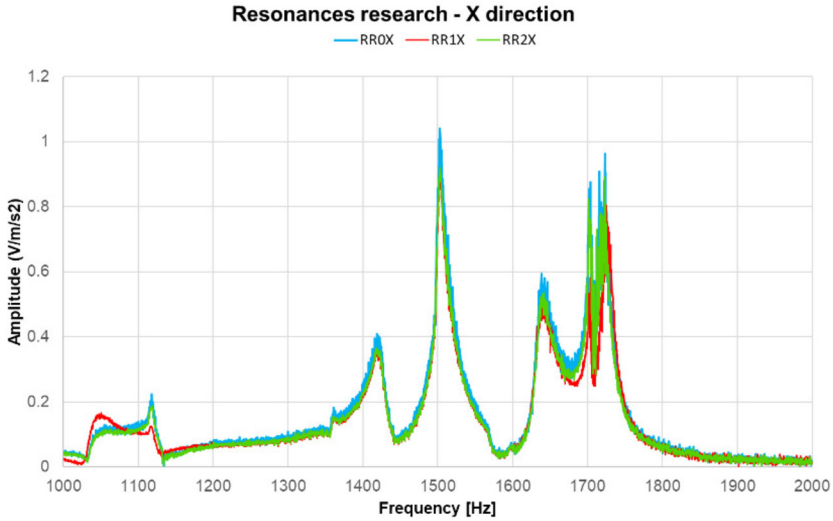

Fig. 9 Resonance search testing IP-1 direction: measured FRF between vibrometer (V units) and accelerometer(m/s^2 units) before sweep sine (sky blue colour), after sweep sine (red colour) and after random (green colour)

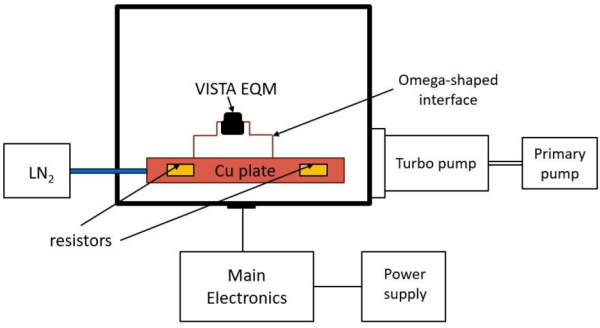

Fig. 10 Vacuum chamber facility schematic

6.2 VISTA Calibration and Functionality Tests

The purpose of the calibration tests is to determine the frequency vs. temperature relationship of the sensor, which is unique for each crystal pair, therefore for each VISTA model. The experimental setup inside the vacuum chamber consists of a copper plate, which can be used as a hot/cold sink and a copper Omega shape to maintain VISTA on the copper plate that can cool and heat the system. On the lateral sides of the plate, 8 aluminium resistors of 10 Ω each are mounted with screws; they are used to heat the plate. Underneath the copper plate, there is a serpentine for liquid nitrogen, in order to cool it down, linked to an external LN_2 dewar. A schematic of the facility is shown in Fig. 10.

The calibration curve of VISTA Flight Model (FM) in the operational temperature range of Milani is shown in Fig. 11. This curve has been obtained in a step-wise manner: the heaters are turned on to reach the set point temperature (from −30 °C to 35 °C); once the set point is reached, the beat frequency and the crystals temperature are monitored for 10 minutes. The mean value and the error bars for the beat frequency are reported in the plot.

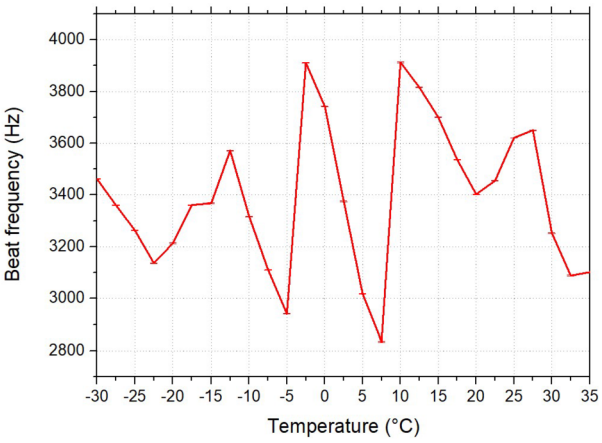

Fig. 11 VISTA FM calibration curve. The error bars for the beat frequency are shown. The maximum oscillation at each set point is ±2 Hz

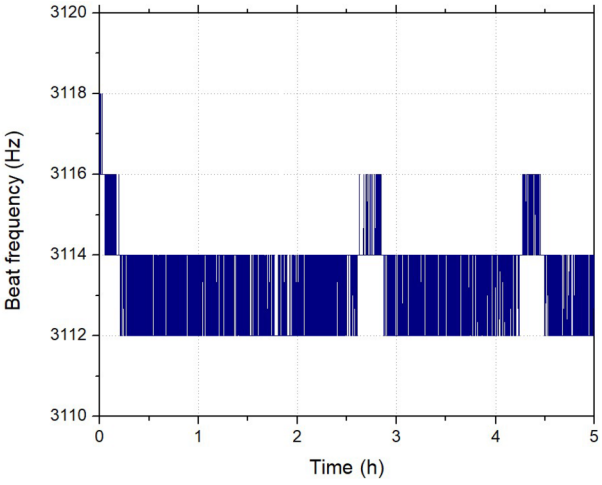

Fig. 12 The sensor frequency vs. time is monitored for 5 hours at 25 °C in vacuum chamber at 10^{-6} mbar. The frequency is 3113.3±1.2 Hz

A possible solution to discriminate between dust accumulation and temperature trends is to operate the instrument preferentially within "less critical" temperature ranges, e.g. between 10 °C and 25 °C, and to perform the accumulation and analysis within this range by activating VISTA subsystems for thermal control.

The functionality tests aim at verifying the temporal stability of frequency, the correct functioning of the Thermal Control System (i.e. built-in heaters and TEC) at different temperature set points. In order to check the lack of temporal drifts of the frequency without external solicitations, the sensor head was placed in vacuum and monitored for 5 hours. The result is shown in Fig. 12.

The functionality of the two thermal subsystems (i.e. heaters and TEC) is assessed by placing the sensor head in the vacuum chamber and heating/cooling the crystals by a fixed ΔT. The temperature rate for both heating and cooling tests is 1 °C/min; the waiting time at each set point is 20 minutes, in order to check the temperature stability (within 0.1 °C) when the heaters or the TEC are set. An example of heating test is shown in Fig. 13, while a cooling test is shown in Fig. 14.

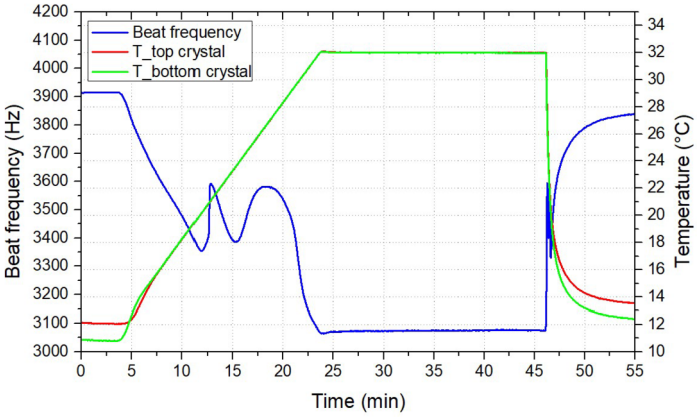

Fig. 13 VISTA is in active mode and the crystals are heated of 20 °C with a slope of 1 °C/min. The crystals temperatures and the frequency are monitored during the waiting time at set point, with the following values: $T_{top} = 32.01 \pm 01$ °C; $T_{bot} = 32.01 \pm 0.01$ °C and $f = 3074.4 \pm 1.6$ Hz respectively

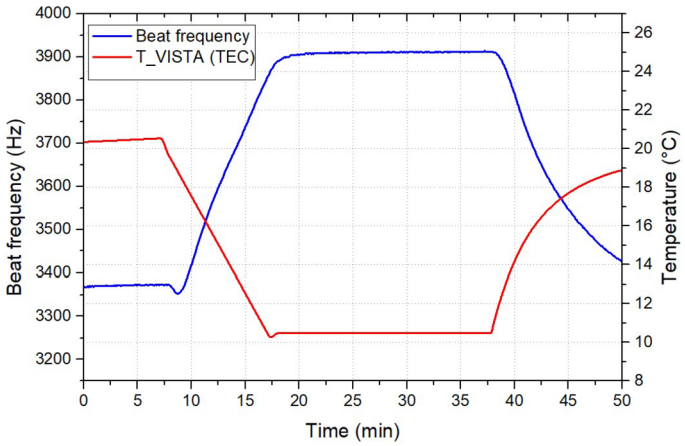

Fig. 14 The sensor is cooled by the TEC of 10 °C with a slope of 1 °C/min and a stabilization time of 20 minutes. The TEC temperature and the frequency are monitored during the waiting time at set point, with the following values of $T_{TEC} = 10.5 \pm 0.01$ °C and $f = 3909.9 \pm 1.6$ Hz, respectively

6.3 VISTA Performance Tests

The performance tests consist of a simulation of particles/volatiles deposition simulation, aimed at verifying the sensor head capability to measure the mass accumulation on the sensing crystal surface (the one exposed to the external environment). The setup used for the performance tests is shown in Fig. 15: an effusing cell containing an organic material is used as the source and placed in the FOV (one to one) of the sensing crystal (Dirri et al. 2016). The path of particles/volatiles flux is focused on the exposed crystal by using a fixed distance (previously calibrated) in order to obtain a reliable flux for the analysis. The copper plate (cold sink) is cooled by means of a LiN_2 serpentine managed with a separate PID, while VISTA is mounted on the Ω-shaped copper. Thus, the sensor head is cooled down and

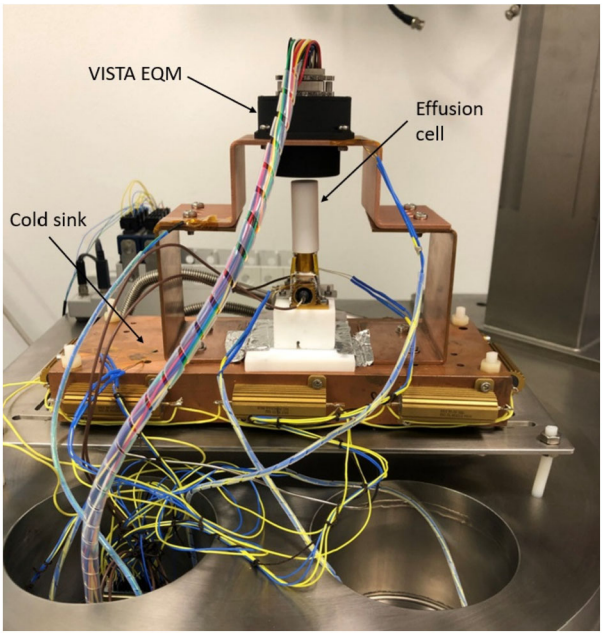

Fig. 15 Performance tests setup: the effusion cell containing an organic compound is used as a contamination source and placed in the FOV of the sensing crystal, in order to focus the flux on particles on it. During the tests, the sensor is cooled down and used as cold finger to increase the condensation of molecules

used as cold finger to increase the condensation of molecules on the crystals surface. The performance tests are performed with the Engineering Qualification Model of VISTA only, to avoid contamination of the flight models.

During the tests, the cold sink is maintained at −10 °C so that VISTA EQM crystals reach −5 °C in order to accumulate molecules. The temperature of the effusion cell is increased during the test (purple curve in Fig. 16) from 50 °C up to 100 °C. The frequency increase (blue curve) indicates the accumulation of material on the sensing crystals while the average deposition rates for each temperature step and the corresponding deposited mass are reported in Table 5.

After the deposition, one TGA cycle is performed (Fig. 17): the crystals are heated up to 50 °C with the built-in heaters to desorb the deposited material. The crystals heating is performed together by using the developed software program to control in real-time the instrument and specific Proportional-Integral-Derivative (PID) values (previously calibrated for the VISTA-Hera crystals couples) to control each ramp rate (from 1 to 10 °C/min).

The initial and final frequency and the desorbed mass are reported in Table 6.

Most of the material desorption happens between 30 and 50 °C, in agreement with the desorption temperatures of dicarboxylic acid used in vacuum (Dirri et al. 2016), while residual mass is ascribed to compound impurities which survived regeneration (this material has a purity of 99%: this means that, even after regeneration, 1% of residues can remain in the crystal). Additional tests were then performed to assess the EQM mass saturation by using the same procedure. The saturation mass of 172.6 μg was measured by heating the effusion cell at maximum 130 °C. This value is crucial to assess the possible saturation of VISTA during the Close Range Phase (CRP).

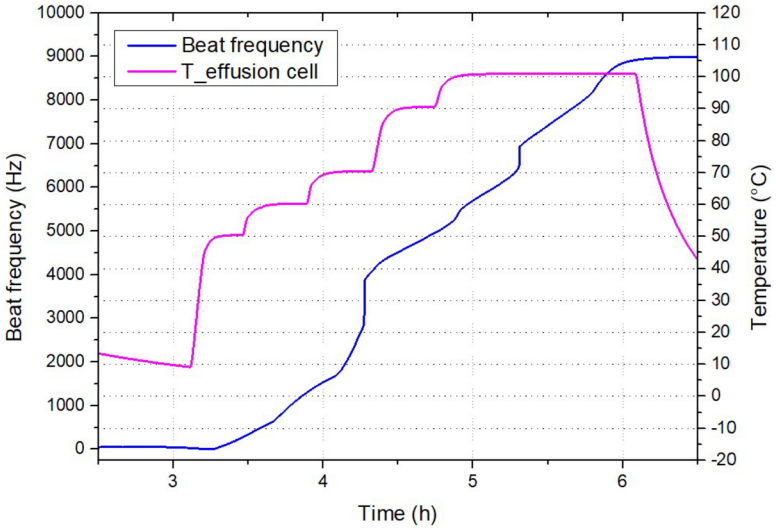

Fig. 16 Performance test: 55 mg of an organic compound (dicarboxylic acid) is placed in effusion cell and heated up to 50, 60, 70, 90 and 100 °C to simulate a deposition process. The deposition rate on sensing crystal varies from 2.8 Hz/min up to 112.6 Hz/min. The initial and final frequencies are 54±3 Hz and 33±2 Hz, respectively

Table 5 VISTA performance test: frequency, average deposition rate and deposited mass

T_{cell} [°C]	Frequency [Hz]	Deposition rate [Hz/s]	Deposited mass [μg]
50	270	0.36	0.27
60	1302	0.75	1.29
70	4094	2.16	3.48
90	4986	0.5	1.10
100	8930	0.82	4.91

7 Conclusion

VISTA payload was developed and tested in three years with the following model philosophy: EM_0, EQM, FM and FS. VISTA FM successfully passed the test campaign and was integrated on Milani Proto-Flight Model (PFM). The sensitive area of VISTA is positioned in the RAM direction in order to increase the possibility to accumulate residual dust from the DART impact (if still present), suspended dust in the binary system or coming from dust levitation process. Thanks to the customized design, VISTA will be able to accomplish the following scientific goals:

- Detection of dust particles smaller than 5-10μm and submicron particles;
- Characterization of volatiles and light organics by means of heating cycles and Thermo-Gravimetric Analysis;
- Molecular contamination assessment in support to other instrumentation on-board Hera mother-spacecraft and Milani payloads, e.g. ASPECT spectrometer.

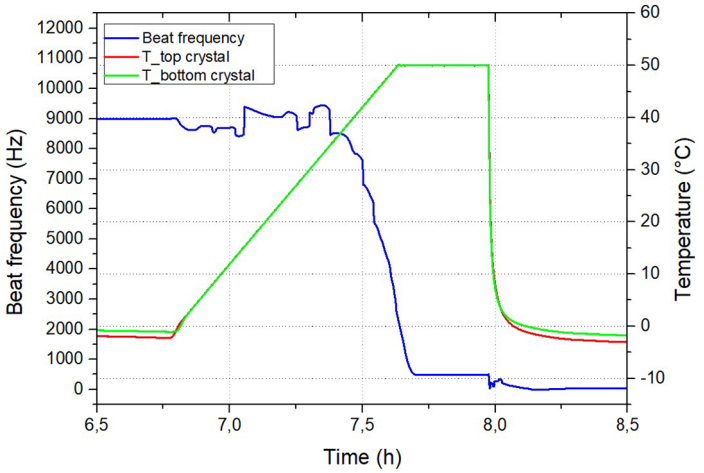

Fig. 17 TGA cycle: the heat sink is kept at 10 °C while the crystals are heated up to 50 °C with a slope of 1 °C/min and a stabilization time of 20 minutes. Most of the deposited mass is desorbed, i.e. the final frequency (54 Hz) is lower than the initial frequency (33 Hz). A residue of the material was remaining on the crystals surface and depends to the compound impurities (1%)

Table 6 TGA after deposition: initial and final values of crystal temperature and frequency, and desorbed mass

T_{start} [°C]	T_{end} [°C]	f_{start} [Hz]	f_{end} [Hz]	Desorbed mass [μg]
−2	50	9002	16	11.19

These scientific goals fall within Milani scientific goal consisting in the characterization of dust particles that may evolve into clouds in the surrounding of Didymos system, as reported in Michel et al. (2022). VISTA Operations in the Far Range Phase (FRP) and Close Range Phase were described and scheduled for Hera cruise and the operational time of Milani CubeSat in the early 2027 (around three months), with a possibility to extend these operations for the landing phase (currently under discussion). Although Milani CubeSat does not fly instruments requiring landing to achieve mission success and scientific return, the Milani mission does foresee an experimental phase upon nominal mission conclusion, aiming at attending a landing on the Dimorphos asteroid for technology demonstration purposes. In that case, VISTA will have the possibility to accumulate dust by scheduling specific fly-bys around Dimorphos and during the possible Milani landing. In this scenario, VISTA will operate in PASSIVE Mode to accumulate dust (< 2 km) and ACTIVE Mode to perform heating cycle (up to 100 °C) and TGA before landing to avoid any problems due to sensor saturation, CubeSat vibrations and impact.

Acknowledgements VISTA Team would like to acknowledge the support received by the whole Milani Consortium and Tyvak International.

Funding Information Open access funding provided by Istituto Nazionale di Astrofisica within the CRUI-CARE Agreement. The development of VISTA was supported by the Italian Space Agency (ASI) (Accordo Attuativo n. 2022-8-HH.0).

Declarations

Competing Interests The authors declare no competing interests.

References

Benson SW, Shaw R (1968) Thermochemistry of oxidation reactions. Adv Chem 75:288–294. https://doi.org/10.1021/ba-1968-0075.ch022

Bottke WF, Moorhead AV, Connolly HC Jr, Hergenrother CW, Molaro JL, Nolan MC, Schwartz SR, Vokrouhlicky D, Walsh KJ, Lauretta DS (2020) Meteoroid impacts as a source of Bennu's particle ejection events. J Geophys Res Planets 125. https://doi.org/10.1029/2019JE006282

Cardi M, Pavoni M, Caldi D et al (2026) The Hera Milani mission: use of a nanosatellite for planetary defence purposes. Space Sci Rev 222

Dirri F, Palomba E, Longobardo A, Zampetti E (2016) Piezoelectric crystal microbalance measurements of enthalpy of sublimation of C_2–C_9 dicarboxylic acids. Atmos Meas Tech 9:655–668. https://doi.org/10.5194/amt-9-655-2016

Dirri F, Palomba E, Longobardo A, Zampetti E, Saggin B, Scaccabarozzi D (2019) A review of quartz crystal microbalances for space applications. Sens Actuators A, Phys 287:48–75. https://doi.org/10.1016/j.sna.2018.12.035

Ferrari F, Fodde I, Piccolo F, et al (2026) The scientific operations of Milani NavCam. Space Sci Rev 222

Hartogh P, Lis DC, Bockelée-Morvan D, Val-Borro M, Biver N, Kuppers M, Emprechtinger M, Bergin EA, Crovisier J, Rengel M, Moreno R, Szutowicz S, Blake GA (2011) Ocean-like water in the Jupiter-family comet 103P/Hartley 2. Nature 478:218–220. https://doi.org/10.1038/nature10519

Langmuir I (1913) The vapour pressure of metallic tungsten. Phys Rev 2:329–342. https://doi.org/10.1103/PhysRev.2.329

Lauretta DS, et al (2019) Episodes of particle ejection from the surface of the active asteroid (101955) Bennu. Science 366. https://doi.org/10.1126/science.aay3544

Michel P, et al (2022) The ESA Hera Mission: detailed characterization of the DART impact outcome and of the binary asteroid (65803) Didymos. Planet Sci J 3. https://doi.org/10.3847/PSJ/ac6f52

Nivens D, Chambers JQ, Anderson TR, White DC (1993) Long-term, on-line monitoring of microbial biofilms using a quartz crystal microbalance. Anal Chem 65. https://doi.org/10.1021/ac00049a013

Palomba E, Poppe T, Colangeli L, Palumbo P, Perrin JM, Bussoletti E, Henning T (2001) The sticking efficiency of quartz crystals for cosmic sub-micron grain collection. Planet Space Sci 49:919–926. https://doi.org/10.1016/S0032-0633(01)00015-0

Palomba E, Colangeli EL, Palumbo P, Rotundi A, Perrin JM, Bussoletti E (2002) Performance of microbalances for dust flux measurement. Adv Space Res 29:1155–1158. https://doi.org/10.1016/S0273-1177(02)00131-X

Palomba E, Longobardo A, Dirri F, Zampetti E, Biondi D, Saggin B, Bearzotti A, Macagnano A (2016) VISTA: a μ-thermogravimeter for investigation of volatile compounds in planetary environments. Orig Life Evol Biosph 46:273–281. https://doi.org/10.1007/s11084-015-9473-y

Sauerbrey G (1959) The use of quartz oscillators for weighing thin layers and for microweighing. Z Phys 155:206–222. https://doi.org/10.1007/BF01337937

Scaccabarozzi D, Saggin B, Tarabini M, Palomba E, Longobardo A, Zampetti E (2014) Thermo-mechanical design and testing of a microbalance for space applications. Adv Space Res 54(11):2386–2397. https://doi.org/10.1016/j.asr.2014.08.030

Scaccabarozzi D, Saggin B, Magni M, Corti MG, Zampetti E, Palomba E, Longobardo A, Dirri F (2021) Calibration in cryogenic conditions of deposited thin-film thermometers on quartz crystal microbalances. Sens Actuators A, Phys 330. https://doi.org/10.1016/j.sna.2021.112878

Scaccabarozzi D, Saggin B, Corti MG, Arrigoni S, Valnegri P, Dirri F, Gisellu C, Palomba E, Longobardo A, Zampetti E (2022) Design of VISTA, a quartz crystal thermogravimetric analyszer for Hera Mission. In: 2022 IEEE 9th international workshop on metrology for AeroSpace. https://doi.org/10.1109/MetroAeroSpace54187.2022.9856401

Wood B, Hall D, Lesho J, Uy O, Dyer J, Bertrand W (1997) MSX satellite flight measurements of contaminant deposition on a CQCM and on TQCMs. In: AIAA, aerospace sciences meeting and exhibit, 35th. https://doi.org/10.2514/6.1997-841

Zampetti E, Pantalei S, Macagnano A, Proietti E, Di Natale C, D'Amico A (2008) Use of a multiplexed oscillator in a miniaturized electronic nose based on a multichannel quartz crystal microbalance. Sens Actuators B, Chem 131:159–166. https://doi.org/10.1016/j.snb.2007.12.011

Zampetti E, Macagnano A, Papa P, Bearzotti A, Petracchini F, Paciucci L, Pirrone N (2017) Exploitation of an integrated microheater on QCM sensor in particulate matter measurements. Sens Actuators A, Phys 264:205–211. https://doi.org/10.1016/j.sna.2017.08.004

Zampetti E, Mancuso MA, Dirri F, Papa P, Capocera A, Bearzotti A, Macagnano A, Scaccabarozzi D (2023) Effects on oscillation amplitude varitions on qcm response to microspheres of different sizes. Sensors 23. https://doi.org/10.3390/s23125682

Authors and Affiliations

Ernesto Palomba[1] · Fabrizio Dirri[1] · Chiara Gisellu[1,2] · Andrea Longobardo[1] · Vincenzo Della Corte[1] · Enrico Nardi[1,2] · Emiliano Zampetti[3] · Cassandra Montiroli[3] · Diego Scaccabarozzi[4] · Marco Giovanni Corti[4] · Bortolino Saggin[5] · Marilena Amoroso[6] · Margherita Cardi[7] · Marco Pavoni[7] · Daniele Calvi[7] · Andrea Zanotti[7] · Filippo Corradino[7] · Fabio Ferrari[8] · Iosto Fodde[8] · Alessia Cremasco[8] · Paolo Panicucci[8] · Michael Küppers[9] · Patrick Michel[10]

✉ E. Palomba
ernesto.palomba@inaf.it

F. Dirri
fabrizio.dirri@inaf.it

C. Gisellu
chiara.gisellu@inaf.it

A. Longobardo
andrea.longobardo@inaf.it

V. Della Corte
vincenzo.dellacorte@inaf.it

E. Nardi
enrico.nardi@inaf.it

E. Zampetti
emiliano.zampetti@cnr.it

C. Montiroli
cassandramontiroli@cnr.it

D. Scaccabarozzi
diego.scaccabarozzi@polimi.it

M.G. Corti
marcogiovanni.corti@polimi.it

B. Saggin
bortolino.saggin@unipd.it

M. Amoroso
marilena.amoroso@asi.it

M. Cardi
margherita@tyvak.eu

M. Pavoni
marco.pavoni@tyvak.eu

D. Calvi
daniele.calvi@tyvak.eu

A. Zanotti
andrea.zanotti@tyvak.eu

F. Corradino
filippo.corradino@tyvak.eu

F. Ferrari
fabio1.ferrari@polimi.it

I. Fodde
iosto.fodde@polimi.it

A. Cremasco
alessia.cremasco@polimi.it

P. Panicucci
paolo.panicucci@polimi.it

M. Küppers
michael.kueppers@esa.int

P. Michel
michelp@oca.eu

1 INAF-IAPS, Via del Fosso del Cavaliere 100, Rome, 00133, Italy

2 Università La Sapienza, Via Eudossiana 18, Rome, 00184, Italy

3 CNR-IIA, Strada Provinciale 35d, Montelibretti, 00010, Italy

4 Politecnico di Milano, Polo Territoriale di Lecco, Via G. Previati 1/C, Lecco, 23900, Italy

5 Dipartimento di Ingegneria Industriale, Università di Padova, Via Venezia 1, Padova, 35121, Italy

6 Agenzia Spaziale Italiana, Via del Politecnico, Rome, 00133, Italy

7 Tyvak International srl, Via Orvieto 19, Turin, 10149, Italy

8 Department of Aeropace Science and Technology, Politecnico di Milano, Via La Masa 34, Milan, 20156, Italy

9 ESAC, European Space Agency, Camino Bajo del Castillo, Urbanización Villafranca del Castillo, Madrid, 28692, Spain

10 Observatoire de la Côte d'Azur, CNRS, Laboratoire Lagrange, Université Côte d'Azur, Nice, France